ELSEVIER

Coordination Chemistry Reviews
208 (2000) 153–167

COORDINATION CHEMISTRY REVIEWS

www.elsevier.com/locate/ccr

Comparison of *o*-benzoquinonediimine with bipyridine and bipyrazine in electronic coupling to ruthenium(II), as a function of spectator ligand

A.B.P. Lever *, S.I. Gorelsky

Department of Chemistry, York University, CCB124, 4700 Keele Street, Toronto, Ont., Canada, M3J 1P3

Received 22 October 1999; accepted 15 December 1999

Contents

Abstract

When comparing $[Ru(LL)_3]^{2+}$ with $[Ru(NH_3)_4(LL)]^{2+}$, the question is raised whether the replacement of the relatively poor LL (LL = 2,2′-bipyridine, 2,2′-bipyrazine or *o*-benzoquinonediimine) π-acceptor and σ-electron ligands by the σ-electron rich ammonia ligands permits a significant improvement in coupling/π-back donation to the remaining LL. Using

* Corresponding author.

PII: S0010-8545(00)00253-8

a ZINDO analysis of the electronic structures of these species, it is shown that 2,2′-bipyridine is unable to accept the extra electron density from the ruthenium center, while *o*-benzoquinonediimine can readily do so. The ligand 2,2′-bipyrazine is slightly more able to accept the electron density than 2,2′-bipyridine.

Keywords: π-Acceptor; σ-Electron; *o*-Benzoquinonediimine; ZINDO; Semi-empirical calculations; Electronic spectra

1. Introduction

Electronic coupling in ruthenium(II) complexes and the prediction of electronic spectra in both mononuclear and dinuclear species has been a topic of considerable topical interest from many groups including, most recently, Zerner and co-workers [1], Hush and co-workers [2–4], Vos and co-workers [5], Boxer and co-workers [6,7], Creutz, Sutin and co-workers [8–12], Broo and Lincoln [13], Sizova and co-workers [14–18], Hoffman, Clarke and co-workers [19], Ferretti and co-workers [20–22] and Launay, Sauvage and co-workers [23] and mostly using INDO/S or variants thereof. We have demonstrated in a series of publications [25–35] that the *o*-benzoquinonediimine fragment (bqdi) is an excellent π-accepting ligand both in the parent species [24–27] and in a series of homologues [28–32]. In a comparison of the parent species $[Ru(LL)_3]^{2+}$ (LL = 2,2′-bipyridine (bpy), 2,2′-bipyrazine (bpz) and bqdi (Scheme 1) back donation can be monitored by the square of the coefficient of the ruthenium 4d(e) contribution to the π* MO, to the lowest lying e symmetry π* orbitals (LUMO + 1,2) of these D_3 species. This increased from 6 to 8 to 21% in the sequence LL = bpy < bpz ≪ bqdi [35].

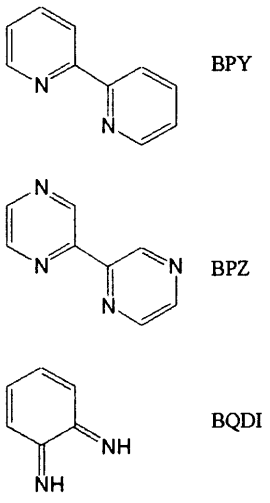

Scheme 1.

Table 1
Comparison of experimental and predicted data for the principal visible region MLCT transition

	Calculated *hv* (f)	Experimental *hv*	Refs.
$[Ru(NH_3)_4(bpy)]^{2+}$	26 300 (0.08)	19 200[a]	[55]
cis-$[Ru(NH_3)_2(bpy)_2]^{2+}$	23 100 (0.19)	20 500[a]	[54]
$[Ru(bpy)_3]^{2+}$	21 700 (0.12); 21 500 (0.08)	22 200[b]	[55]
$[Ru(NH_3)_4(bpz)]^{2+}$	24 500 (0.05)	Unknown compound	
cis-$[Ru(NH_3)_2(bpz)_2]^{2+}$	22 600 (0.16)	Unknown compound	
$[Ru(bpz)_3]^{2+}$	22 000(0.11); 21 400 (0.05)	22 800[b]	[56]
$[Ru(NH_3)_4(bqdi)]^{2+}$	22 700 (0.47)	21 300[b]	[29]
trans-$[Ru(NH_3)_2(bqdi)_2]^{2+}$	22 300 (0.08); 16 900 (0.83)	Unknown compound	
cis-$[Ru(NH_3)_2(bqdi)_2]^{2+}$	18 100 (0.66)	Unknown compound	
$[Ru(bqdi)_3]^{2+}$	18 300 (0.50); 15 500 (0.13)	20 600, 15 200[c]	[57]

[a] Data collected in water; agreement between calculated and experimental data is poor due to solvent effect.
[b] Data collected in acetonitrile.
[c] Datum collected in methanol.

Table 2
Percentage Ru contributions to frontier molecular orbitals

	HOMO-2	HOMO-1	HOMO	LUMO	LUMO+1
$[Ru(NH_3)_4(bpy)]^{2+}$	95 σ	83 π	84 δ	3.5 π	1 δ
$[Ru(bpy)_3]^{2+}$	79	72 (e)	72 (e)	0	7 (e)
$[Ru(NH_3)_4(bpz)]^{2+}$	95 σ	82 π	80 δ	6 π	2 δ
$[Ru(bpz)_3]^{2+}$	71 (e)	71(e)	76.5	0	8.5 (e)
$[Ru(NH_3)_4(bqdi)]^{2+}$	93 σ	61 π	58 δ	20 π	1
trans-$[Ru(NH_3)_2(bqdi)_2]^{2+}$	93 σ	67 π	55 δ	0.4	24 π
cis-$[Ru(NH_3)_2(bqdi)_2]^{2+}$	62	61	58	10	21.5
$[Ru(bqdi)_3]^{2+}$	50.5 (e)	50.5 (e)	60.5	0	21 π

Table 3
Intra-ligand π*–π* coupling energies (cm^{-1})[a,b]

Complex	Coupling energy
cis-$[Ru(NH_3)_2(bpy)_2]^{2+}$	1020
$[Ru(bpy)_3]^{2+}$	1660
cis-$[Ru(NH_3)_2(bpz)_2]^{2+}$	1060
$[Ru(bpz)_3]^{2+}$	2100
cis-$[Ru(NH_3)_2(bqdi)_2]^{2+}$	3840
trans-$[Ru(NH_3)_2(bqdi)_2]^{2+}$	8800
$[Ru(bqdi)_3]^{2+}$	6230

[a] Splitting between π* MOs.
[b] The *trans*-$[Ru(NH_3)_2(LL)]^{2+}$, LL = bpy, bpz are excluded because the LL rings are distorted due to steric hindrance.

Another qualitative probe of the interaction of the metal 4d shell with the π* orbitals is the energy separation between the a_2 and e symmetry π* orbitals of the $(LL)_3$ set. If there were no metal interaction, the three π* orbitals (one on each LL, of equal energy since the ligands are equivalent) could only couple through space and this would generate a splitting of the order of 0.1 eV. In fact the splitting increases from 0.23 to 0.28 to 0.78 eV in the same sequence as above [35].

Yet another measure of delocalization is the magnitude of the quantum mechanical exchange energy, K [36–38], which may be derived from the singlet and triplet metal to ligand charge transfer (MLCT) transition energies of specific Ru $d \rightarrow \pi^*$ transitions. In such a transition, if there is no mixing between the specific d orbital from which the electron is excited and the π* MO into which it goes, then there is a net electron transfer and the time average distance of the electron in the excited state from the filled d orbitals in ground state will generally be large. Since K decreases exponentially with this distance, it will be small. Conversely, if the specific d orbital is mixed with the π* orbital involved in the transition, then the electron in the excited state will spend some time back on the metal, the time average distant apart will be small, and K will be large. Thus, the magnitude of K is a qualitative measure of the extent of delocalization of a specific d orbital over a specific π* ligand orbital. A preliminary analysis of this has been reported [35] and we discuss it in more detail below.

Table 4
Variation in exchange, $2K$ and Coulomb J parameters (cm^{-1}) with symmetry[a]

	π-$2K$, J	δ-$2K$, J	σ-$2K$, J
$[Ru(NH_3)_4(bpy)]^{2+}$	**4160**, 30 500	**1480**, 30 500	**310**, 29 400
$[Ru(bpy)_3]^{2+}(^1E(1))$[b]	**1460**, 27 900		
$[Ru(NH_3)_4(bpz)]^{2+}$	**6400**, 32 350	**2050**, 32 550	**600**, 31 250
$[Ru(bpz)_3]^{2+}$ $(^1E(1))$[b]	**1540**, 28 500		
$[Ru(NH_3)_4(bqdi)]^{2+}$	**17 700**, 39 250	**6500**, 38 200	**1900**, 36 750
trans-$[Ru(NH_3)_2(bqdi)_2]^{2+}$	**9000**, 31 000	**3850**, 35 600	**2300**, 37 200
$[Ru(bqdi)_3]^{2+}$ $(^1E(1))$[b]	**5415**, 29 600		

[a] The δ- and σ-data are undefined for the $[Ru(LL)_3]^{2+}$ species.
[b] See Table 5 and footnotes therein.

Table 5
Variation in exchange, $2K$ and Coulomb J parameters (cm^{-1}) with ligand in the $[Ru(LL)_3]^{2+}$ series as a function of electronic state

State[a]	LL = Bipyridine, $2K$, J	LL = Bipyrazine, $2K$, J	LL = BQDI, $2K$, J
$A_2(1)$	**630**, 28 300	**680**, 28 800	**2000**, 29 850
E(1)	**1460**, 27 900	**1540**, 28 500	**5415**, 29 600
E(2)	**1100**, 30 100	**1270**, 30 950	**2960**, 33 850

[a] Excitations giving rise to states are: $A_2(1)$, $a_1 \rightarrow a_2$; E(1), $e \rightarrow a_2$; E(2), $a_1 \rightarrow e$. Analysis of $e \rightarrow e$ transitions is excluded, see Ref. [58].

Table 6
Orbital energies and mixing in $[Ru(bpy)_3]^{2+}$

MO number	Eigenvalue (eV)	Ru (%)	bpy (%)
100	−4.271	0.2	99.8
99	−5.034	1.3	98.7
98	−5.034	1.3	98.7
97	−5.225	0.0	100.0
96	−5.393	2.7	97.3
95	−5.414	0.7	99.3
94	−5.414	0.7	99.3
93	−6.193	6.8	93.2
92	−6.193	6.8	93.2
91 L	−6.398	0.1[a]	99.9
90 H	−12.401	72.3	27.7
89	−12.401	72.3	27.7
88[b]	−12.426	79.6	20.4
87	−13.924	0.5	99.5
86	−13.924	0.5	99.5
85[b]	−14.034	2.0	98.0
84	−15.547	0.4	99.6
83	−15.547	0.4	99.6
82	−15.554	0.1	99.9
81	−15.636	0.0	100.0
80	−15.636	0.0	100.0

[a] An a_2 symmetry wavefunction; in D_3 symmetry, the $4d(t_{2g})$ metal contribution would be zero. The contribution indicated refers to the Ru $5p_z$ (a_2) orbital.

[b] a_1 symmetry wavefunctions. In all these tables the Ru content reflects the total 5s, 5p and 4d contribution, but the 5s and 5p components are very small.

The earlier comparative analysis [35] investigated species of the type $[Ru(LL')_{3-n}(LL)_n]^{2+}$ where LL′ and LL were the above ligands and also azodipyridine. This presented a competitive situation were delocalization over both LL′ and LL could occur. In this Note we explore species of the type $[Ru(NH_3)_{6-2n}(LL)_n]^{2+}$ to remove this competition and to ask the question 'does back donation/delocalization increase substantially, as the electron richness of the ruthenium center increases with increasing number of bound ammonia residues?'

2. Methodology

We have used the ZINDO method (modified INDO) [39–45] to understand these complexes. This method gives excellent predictions of trends in electronic transition energies and good predictions of absolute band energies for visible region bands [28,29,35,46–52]. Our application of this method has been discussed previously [28,30,34,35] and is only summarized here.

2.1. Geometry optimization

Structures of all the complexes were derived using the modified INDO/L semiempirical method (ZINDO/L) using the developmental version of ZINDO running on an SGI Origin 2000 computer. The convergence gradient was lower than 30 cal mol^{-1} $Å^{-1}$. The recommended value of the 'resonance' integral parameter for Ru, $\beta(4d) = -26.5$ eV [53] overestimates the Ru–N bond strength yielding rather short Ru–N distances. A value of $\beta(4d) = -20$ eV was used [35]. In addition, we adjusted the equatorial and axial Ru–NH_3 distances to 214 and 216 pm, respectively, to agree with literature X-ray data. Using somewhat shorter distances had very little impact on the data and no impact on the conclusions. All other ZINDO/L parameters were the default parameters in the program. The bond lengths and angles in the geometry optimized structures are consistent with X-ray data for complexes of this type. (see website for xyz files).

2.2. Molecular orbital energies, coefficients and electronic spectra calculations

These were obtained using the modified INDO/S (ZINDO/S) method in the Hyperchem program, and incorporating the Ru INDO/S parameter set obtained by Krogh-Jespersen et al. [50]. Other atomic parameters were the default parameters of the Hyperchem program. The SCF convergence tolerance was 10^{-4} kcal mol^{-1}.

Table 7
Orbital energies and mixing in *cis*-$[Ru(NH_3)_2(bpy)_2]^{2+}$

MO Number	Eigenvalue (eV)	Ru (%)	NH_3 (%)	bpy (%)
80	−3.174	0.2	0.1	99.7
79	−3.764	33.9	5.4	60.7
78	−3.839	47.4	16.3	36.4
77	−4.595	0.0	0.0	100.0
76	−4.615	0.1	0.0	99.9
75	−5.405	1.0	0.0	99.0
74	−5.530	0.3	0.1	99.6
73	−5.787	1.9	0.0	98.0
72	−5.804	0.5	0.0	99.5
71	−6.605	6.5	0.2	93.2
70 L	−6.731	2.1	0.3	97.6
69 H	−12.942	76.4	1.5	22.1
68	−13.070	82.1	0.8	17.2
67	−13.108	83.8	0.9	15.2
66	−14.290	0.9	0.0	99.1
65	−14.356	2.2	0.0	97.8
64	−15.927	0.3	0.0	99.6
63	−15.988	0.3	1.1	98.7
62	−16.141	0.4	0.0	99.6
61	−16.373	5.8	1.2	93.0
60	−16.380	6.1	0.8	93.0

Table 8
Orbital energies and mixing in $[Ru(NH_3)_4(bpy)]^{2+}$

MO number	Eigenvalue (eV)	Ru (%)	NH_3 (%)	bpy (%)
55	−3.642	0.1	0.0	99.9
54	−4.528	47.4	15.5	37.0
53	−4.800	62.7	30.3	7.0
52	−5.103	0.1	0.0	99.9
51	−5.965	0.4	0.1	99.5
50	−6.293	0.9	0.0	99.0
49 L	−7.208	3.0	0.3	96.7
48 H	−13.868	85.5	2.4	12.1
47	−13.873	84.4	2.4	13.2
46	−13.995	95.2	2.4	2.4
45	−14.834	2.7	0.1	97.3
44	−16.549	0.3	0.1	99.7
43	−16.842	5.7	0.7	93.6
42	−16.908	7.4	2.9	89.7
41	−18.002	4.3	4.1	91.6
40	−18.200	5.6	8.0	86.3
39	−19.550	1.0	5.7	93.3
38	−19.585	1.0	1.7	97.3
37	−20.348	5.8	72.2	22.0
36	−20.478	3.4	27.3	69.3
35	−20.528	1.6	4.5	93.9

Electronic spectra included single excitation configuration interaction (CIS) [37]. The number of configurations used was generally ca. 1800 (e.g. ca. 30 × 30 occupied × unoccupied orbitals). An increase in the number of configurations had little effect on the predicted visible region absorption energies. The overlap weighting factors σ–σ and π–π were set at 1.267 and 0.585, respectively. Oscillator strengths were calculated in the dipole length approximation including the one-center sp and pd atomic terms.

2.3. Calculation of J and K

Configurational interaction was not used since it was important to obtain energies of the un-mixed excited states. Thus, the excitation energies of the transitions of each of the three $4d(t_{2g})$ orbitals to the LUMO π* orbital localized mainly on the ligand LL were calculated to generate the six excited spin singlet and triplet states. In these closed shell Ru(II) species, the difference between the singlet and triplet state energies for each excitation is equal to $2K$ [37,38,45]. The magnitude of the Coulomb potential, J, can then be derived from the expression:

$$h\nu(\text{singlet}) = E_{\pi^*} - E_d - J + 2K \quad (1)$$

where E_{π^*} and E_d are the orbital energies of the acceptor LUMO and donor d orbital, respectively [37,38,45]. When degenerate orbitals are involved, one-electron

excitation can give rise to several excited states. This situation is met in the $[Ru(LL)_3]^{2+}$ species and is discussed in more depth below.

3. Results and discussion

3.1. d-Orbital mixing

We explore delocalization in the series $[Ru(NH_3)_{6-2n}(LL)_n)]^{2+}$. Note that the *trans*-$[Ru(NH_3)_2(LL)_2]^{2+}$ species, LL = bpy, bpz are omitted since the LL ligands are buckled by steric interference. In all the species under investigation, the LUMO is mostly localized on the LL π* orbital and the HOMO, HOMO-1 and HOMO-2 are mostly the $4d(t_{2g})$ Ru set. However, in some cases, these d orbitals are dispersed over several additional π and π* ligand orbitals.

In the LL = bpy and bpz complexes, the Ru $4d(t_{2g})$ set can readily be identified in these Tables as HOMO, HOMO-1 and HOMO-2 having predominantly Ru character. In these specific species; the most mixed is $[Ru(bpz)_3]^{2+}$, but even here the Ru character does not drop below 71% (Tables 6–11).

Table 9
Orbital energies and mixing in $[Ru(bpz)_3]^{2+}$

MO number	Eigenvalue (eV)	Ru (%)	bpz (%)
100	−4.973	0.0	100.0
99	−5.751	0.5	99.5
98	−5.751	0.5	99.5
97	−5.901	0.0	100.0
96	−6.522	3.6	96.4
95	−6.571	1.5	98.5
94	−6.571	1.5	98.5
93	−7.211	8.6	91.4
92	−7.211	8.6	91.4
91 L	−7.471	0.1[a]	99.9
90 H[b]	−13.513	76.5	23.5
89	−13.545	71.2	28.8
88	−13.545	71.2	28.8
87	−14.458	1.9	98.1
86	−14.458	1.9	98.1
85[b]	−14.590	5.8	94.2
84	−16.105	0.3	99.7
83	−16.105	0.3	99.7
82	−16.137	0.2	99.8
81	−16.163	0.4	99.6
80	−16.208	1.4	98.6

[a] An a_2 symmetry wavefunction; in D_3 symmetry, the metal d contribution is zero. This contribution is from Ru p_z.

[b] a_1 symmetry wavefunctions.

Table 10
Orbital energies and mixing in *cis*-$[Ru(NH_3)_2(bpz)_2]^{2+}$

MO number	Eigenvalue (eV)	Ru (%)	NH_3 (%)	bpz (%)
80	−3.868	0.2	0.0	99.8
79	−4.388	37.9	5.9	56.2
78	−4.542	51.0	16.9	32.1
77	−5.145	0.0	0.0	100.0
76	−5.172	0.0	0.0	100.0
75	−5.972	0.4	0.0	99.5
74	−6.066	0.1	0.0	99.8
73	−6.762	3.1	0.0	96.8
72	−6.812	0.9	0.0	99.0
71	−7.478	8.3	0.3	91.4
70 L	−7.612	3.6	0.3	96.2
69 H	−13.822	74.9	1.4	23.8
68	−13.947	81.1	0.9	18.1
67	−13.968	80.8	0.9	18.3
66	−14.691	2.8	0.0	97.2
65	−14.774	6.5	0.1	93.3
64	−16.322	0.3	0.1	99.7
63	−16.328	0.4	0.1	99.5
62	−16.449	0.6	0.7	98.7
61	−16.451	1.3	0.1	98.6
60	−16.556	0.6	0.4	99.0

For LL = bqdi, on the other hand, the Ru content of this group of three orbitals can drop to as low as 50% and there are several other orbitals with substantial Ru character (see Tables 12–15). Table 1 compares the experimentally observed principal intense visible region MLCT band with the predicted energy. However, not all the complexes have been reported in the literature. It is not the intent of this article to discuss these electronic spectra, but solely to show that the theory reproduces the available experimental data in a satisfactory manner.

Table 2 reveals the percentage 4d metal contribution (square of coefficient normalized to 100%) being data abstracted from the more extensive listing in Tables 6–15. With the exception of the $[Ru(LL)_3]^{2+}$ and *cis*-$[Ru(NH_3)_4(LL)_2]^{2+}$ species, the symmetry is axial and it is possible to distinguish the d orbitals which are σ-, δ- and π- with respect to the LL plane. In these axial cases, the $4d(t_{2g})$ σ-orbital remains fairly pure (unmixed). The δ– and π–d orbitals are more extensively mixed with ligand orbitals, and to a similar degree. The conclusion which may be drawn reflects our earlier picture that the π-accepting character of these species increases in the sequence bpy < bpz ≪ bqdi. Irrespective of which homologous series we consider, the 'purity' of the $4d(t_{2g})$ set decreases in that sequence. This is true for each value of '*n*', but is most marked in the $[Ru(LL)_3]^{2+}$ series ($n = 3$) where the e pair from $4d(t_{2g})$ is most strongly affected by interaction both with filled π and empty π* ligand orbitals of e symmetry. The a_1 orbital (HOMO in $Ru(bqdi)_3]^{2+}$) is also significantly mixed (but less so than e) through interaction with a lower but

closely lying filled π-orbital of a_1 symmetry (see Table 12). This is also true, but to a much less extent for the $[Ru(bpz)_3]^{2+}$ species (Table 9, orbitals # 85,91), but such mixing is largely absent for LL = bpy, $n = 3$ (Table 6).

Back donation to the low lying ligand π* orbitals also falls into the same sequence for each series. However, it is revealing to consider the average back-donation per ligand by dividing the percentage mixing by the number of LL ligands in the complex. The question then arises whether decreasing the number of LL ligands and increasing the electron richness of the ruthenium by replacing LL with 2 NH_3 molecules, leads to increased back donation to the remaining LL ligands. Can the LL ligand take advantage of the extra electron richness? For bpy, consideration of the data in Table 2 shows that the back donation per bpy ligand is essentially independent of '*n*', the number of LL ligands. Thus, the bipyridine ligand is incapable of adapting to the more electron rich Ru atom by accepting more π-electron density. For bpz, there is a slight increase in back-donation with decreasing '*n*', and so bpz can adapt to a limited degree. For bqdi however, there is a dramatic increase in *back-donation per LL* ligand increasing from 7% to 10–12 to 20% in the sequence $[Ru(bqdi)_3]^{2+}$, *cis*- and *trans*-$[Ru(NH_3)_2(bqdi)_2]^{2+}$ and finally to $[Ru(NH_3)_4(bqdi)]^{2+}$. Thus, by this criterion, bqdi can readily adapt to the extra electron richness and will delocalize more electron density off the metal center.

Table 11
Orbital energies and mixing in $[Ru(NH_3)_4(bpz)]^{2+}$

MO number	Eigenvalue (eV)	Ru (%)	NH_3 (%)	bpz (%)
60	−3.091	7.9	4.1	88.0
59	−3.373	19.9	8.3	71.8
58	−3.607	40.8	36.8	22.4
57	−3.748	0.2	0.0	99.8
56	−3.895	9.1	5.5	85.5
55	−4.169	0.2	0.0	99.7
54	−4.811	44.4	15.4	40.2
53	−5.241	62.2	30.4	7.4
52	−5.474	0.0	0.0	100.0
51	−6.326	0.3	0.0	99.7
50	−7.113	1.9	0.0	98.1
49 L	−7.888	6.1	0.5	93.4
48 H	−14.348	79.9	2.3	17.8
47	−14.409	82.3	2.4	15.3
46	−14.481	94.7	2.3	2.9
45	−15.068	8.2	0.2	91.6
44	−16.617	0.4	0.6	99.0
43	−16.784	0.6	0.9	98.6
42	−16.856	1.0	0.2	98.8
41	−18.263	4.8	1.1	94.1
40	−18.341	5.1	5.4	89.5

Table 12
Orbital energies and mixing in $[Ru(bqdi)_3]^{2+}$

MO number	Eigenvalue (eV)	Ru (%)	bqdi (%)
75	−3.440	1.1	98.9
74	−4.188	40.6	59.4
73	−4.188	40.6	59.4
72	−4.887	0.8	99.2
71	−4.887	0.8	99.2
70	−4.913	0.0	100.0
69	−5.115	0.9	99.1
68	−5.135	0.3	99.7
67	−5.135	0.3	99.7
66	−7.880	21.0	79.0
65	−7.880	21.0	79.0
64	−8.650	0.1[a1]	99.9
63 H[b1]	−13.514	60.5	39.5
62	−13.666	50.5	49.5
61	−13.666	50.5	49.5
60	−14.719	6.5	93.5
59	−14.719	6.5	93.5
58[b1]	−15.100	22.3	77.7
57	−16.826	0.2	99.8
56	−17.292	5.8	94.2
55	−17.292	5.8	94.2

[a] An a_2 symmetry wavefunction; in D_3 symmetry, the metal d contribution is zero. This contribution is from Ru p_z.
[b] a_1 symmetry wavefunctions.

3.2. $\pi^*-\pi^*$ Coupling

Table 3 shows the energy separation between the two lowest lying π* orbitals on the collective ligands. For each homologous series, this increases in the sequence bpy < bpz ≪ bqdi, and is a maximum in the species *trans*-$[Ru(NH_3)_2(bqdi)_2]^{2+}$ where a single d orbital can bind to the out-of phase $\pi^*-\pi^*$ combination and destabilize it with respect to the in-phase combination, which cannot interact with a Ru d-orbital (but can with a Ru p-orbital).

3.3. Analysis of the exchange and Coulomb potentials

Table 4 shows the values of $2K$ and J for the various complexes. The same pattern emerges. There is an overall increase in $2K$ for each series from bpy to bpz to bqdi. The transitions from the σ-orbitals generate the smallest $2K$ values as expected. While the mixing coefficients are rather similar for the δ- and π–d-orbitals, the $2K$ values are seen to be significantly higher for the π-type transitions than for the δ.

This arises because the π-type transitions (in *trans*-$[Ru(NH_3)_2(LL_{)2}]^{2+}$ and $[Ru(NH_3)_4(LL)]^{2+}$) occur between orbitals in which the d orbital from which

excitation occurs, is identically the same as the d orbital which couples to the π* orbital into which excitation proceeds. This is never true for the δ-type excitation.

The $2K$ values for the bqdi complexes, especially $[Ru(bqdi)_3]^{2+}$ ($^1A_1$ state) and $[Ru(NH_3)_4(bqdi)]^{2+}$ are dramatically large indicating thereby extensive delocalization. Note that the $2K$ values for $[Ru(LL)_3]^{2+}$ (LL = bpy, bpz) are also fairly large, but that, unlike for LL = bqdi, passing to $[Ru(NH_3)_4(LL)]^{2+}$ the $2K$ values decrease significantly, supporting the above view that these ligands cannot take advantage of the extra electron richness of the Ru center.

In D_3 symmetry, the π-type transition involves an $e \rightarrow e$ transition giving rise to $A_1 + A_2 + E$ states. Taking into account the other $d \rightarrow \pi^*$ transitions (into $\pi^*(a_2 + e)$), there are six possible MLCT transitions, A_1, $2 \times A_2$ and $3 \times E$ each of which gives rise to spin singlet and triplet states. The $2K$ values for each (unscrambled) state can be determined [58] and these are shown in Table 5. Data are in general agreement for LL = bpy from a density functional theory study [59].

The Coulomb J values depend inversely on the time average distance of the excited electron from the Ru center and are less sensitive to delocalization. The J values for the σ-type MLCT bands tend to be lower than the δ- and π-type, but otherwise there is little variation (Table 4).

In conclusion, these studies confirm the view that bqdi is a much better π-acceptor than either bpy or bpz and that it is capable of increasing the extent of delocalization with increasing electron richness of the ruthenium center. We have

Table 13
Orbital energies and mixing in *cis*-$[Ru(NH_3)_2(bqdi)_2]^{2+}$

MO number	Eigenvalue (eV)	Ru (%)	NH_3 (%)	bqdi (%)
60	−3.616	3.1	2.2	94.7
59	−4.563	44.7	5.9	49.4
58	−4.865	53.6	18.0	28.5
57	−5.135	0.8	0.1	99.1
56	−5.161	0.6	0.2	99.1
55	−5.393	0.9	0.0	99.1
54	−5.408	0.6	0.1	99.3
53	−8.212	21.5	0.7	77.7
52 L	−8.688	9.9	0.7	89.4
51 H	−13.909	58.1	1.0	40.9
50	−14.067	61.4	0.8	37.8
49	−14.214	61.9	0.8	37.3
48	−15.019	12.8	0.3	86.9
47	−15.287	24.3	0.6	75.0
46	−17.334	3.8	1.8	94.3
45	−17.799	10.2	1.8	88.0
44	−18.084	2.2	0.9	96.9
43	−18.206	2.0	0.8	97.2
42	−18.452	5.2	0.8	94.1
41	−18.803	4.2	4.2	91.5
40	−18.908	9.0	2.0	89.0

Table 14
Orbital energies and mixing in *trans*-$[Ru(NH_3)_2(bqdi)_2]^{2+}$

MO number	Eigenvalue (eV)	Ru (%)	NH_3 (%)	bqdi (%)
60	−3.781	1.3	0.0	98.6
59	−4.324	33.4	0.0	66.5
58	−5.056	59.7	27.2	13.1
57	−5.187	0.9	0.0	99.1
56	−5.233	0.2	0.1	99.8
55	−5.415	1.1	0.0	98.9
54	−5.513	0.1	0.0	99.9
53	−7.917	24.3	0.2	75.5
52 L	−9.009	0.4	1.3	98.4
51 H	−13.592	64.6 δ*	0.9	34.5
50	−14.043	56.7 π*	0.9	42.4
49	−14.232	93.3	0.1	6.7
48	−14.935	0.1	0.0	99.9
47	−15.360	19.6 δ	0.7	79.7
46	−17.269	0.0	6.3	93.7
45	−17.855	10.4 π	1.4	88.2
44	−17.977	2.3	0.5	97.2
43	−18.355	0.1	0.1	99.9
42	−18.493	4.7	1.3	94.0
41	−18.516	2.3	0.9	96.8
40	−18.876	11.3 δ	3.5	85.2

Table 15
Orbital energies and mixing in $[Ru(NH_3)_4(bqdi)]^{2+}$

MO number	Eigenvalue (eV)	Ru (%)	NH_3 (%)	bqdi (%)
48	−2.652	17.9	81.2	1.0
47	−3.434	0.1	0.0	99.9
46	−3.740	9.0	7.9	83.1
45	−3.794	55.4	38.2	6.4
44	−4.715	46.4	16.5	37.1
43	−5.372	0.5	0.0	99.4
42	−5.581	61.4	30.8	7.8
41	−5.659	0.6	0.0	99.4
40 L	−8.685	20.1 π*	1.2	78.7
39 H	−14.241	57.7 δ*	1.3	41.0
38	−14.628	61.4 π*	1.7	36.9
37	−14.850	93.0 σ*	2.2	4.8
36	−15.564	27.7 δ	1.0	71.3
35	−17.969	10.9 π	3.7	85.4
34	−18.467	2.4	3.0	94.6
33	−19.204	9.0 δ	3.0	88.0
32	−19.211	5.0	6.1	88.9
31	−20.219	4.1	17.4	78.6
30	−20.603	5.2	56.5	38.3
29	−20.737	5.3	45.1	49.6
28	−21.910	5.7	51.5	42.7
27	−22.347	6.8	39.7	53.5

demonstrated that d–π* mixing coefficients, π*–π* splitting of equivalent orbitals and $2K$ integrals can all be used to assess the extent of electronic coupling between metal and ligand and that all give qualitatively the same picture.

Website: note that the structures for all the species, as xyz files, can be found on our web site and can be viewed with CHIME software. Visit http://www.chem.yorku.ca/profs/lever and follow links to this paper.

Acknowledgements

We are indebted to the Natural Sciences and Engineering Research Council for financial support. S.I.G. thanks the Province of Ontario for a Graduate Fellowship.

References

[1] K.K. Stavrev, M.C. Zerner, T.J. Meyer, J. Am. Chem. Soc. 117 (1995) 8684.
[2] J. Zeng, N.S. Hush, J.R. Reimers, J. Am. Chem. Soc. 118 (1996) 2059.
[3] J. Zeng, N.S. Hush, J.R. Reimers, J. Phys. Chem. 100 (1996) 19292.
[4] J. Zeng, N.S. Hush, J.R. Reimers, J. Phys. Chem. 99 (1995) 10459.
[5] T.E. Keyes, R.J. Forster, P.M. Jayaweera, C.G. Coates, J.J. McGarvey, J.G. Vos, Inorg. Chem. 37 (1998) 5925.
[6] S.G. Boxer, R.A. Goldstein, D.J. Lockhart, T.R. Middendorf, L. Takiff, J. Phys. Chem. 93 (1989) 8280.
[7] D.H. Oh, M. Sano, S.G. Boxer, J. Am. Chem. Soc. 113 (1991) 6880.
[8] Y.G.K. Shin, B.S. Brunschwig, C. Creutz, M.D. Newton, N. Sutin, J. Phys. Chem. 100 (1996) 1104.
[9] Y.K. Shin, B.S. Brunschwig, C. Creutz, N. Sutin, J. Phys. Chem. 100 (1996) 8157.
[10] Y.K. Shin, B.S. Brunschwig, C. Creutz, N. Sutin, J. Am. Chem. Soc. 117 (1995) 8668.
[11] Y.K. Shin, D.J. Szalda, B.S. Brunschwig, C. Creutz, N. Sutin, Inorg. Chem. 36 (1997) 3190.
[12] B.S. Brunschwig, C. Creutz, N. Sutin, Coord. Chem. Rev. 177 (1998) 61.
[13] A. Broo, P. Lincoln, Inorg. Chem. 36 (1997) 2544.
[14] O.V. Sizova, V.I. Baranovskii, N.V. Ivanova, A.I. Panin, Int. J. Quant. Chem. 65 (1997) 183.
[15] O.V. Sizova, V.I. Baranovskii, N.V. Ivanova, A.I. Panin, J. Struct. Chem. 37 (1996) 525.
[16] O.V. Sizova, N.V. Ivanova, V.I. Baranovskii, A.B. Nikolskii, Russ. J. Struct. Chem. 35 (1994) 12.
[17] O.V. Sizova, V.I. Baranovskii, A.I. Panin, N.V. Ivanova, J. Struct. Chem. 39 (1998) 471.
[18] O.V. Sizova, N.V. Ivanova, V.I. Baranovskii, A.I. Panin, Koord. Khim. 22 (1996) 591.
[19] K.J. LaChance-Galang, P.E. Doan, M.J. Clark, U. Rao, A. Yamano, B.M. Hoffman, J. Am. Chem. Soc. 117 (1995) 3529.
[20] A. Ferretti, A. Lami, G. Villani, Inorg. Chem. 37 (1998) 2799.
[21] I. Cacelli, A. Ferretti, J. Phys. Chem. A 103 (1999) 4438.
[22] A. Ferretti, A. Lami, L.F. Murga, I.A. Shehadi, M.J. Ondrechen, G. Villani, J. Am. Chem. Soc. 121 (1999) 2594.
[23] C. Patoux, C.J.P. Launay, M. Beley, M.K.S. Chodorowski, J.P. Collin, J.P.S. James, J.P. Sauvage, J. Am. Chem. Soc. 120 (1998) 3717.
[24] H. Masui, A.B.P. Lever, Inorg. Chem. 32 (1993) 2199.
[25] H. Masui, A.B.P. Lever, P.R. Auburn, Inorg. Chem. 30 (1991) 2402.
[26] H. Masui, A.B.P. Lever, E.S. Dodsworth, Inorg. Chem. 32 (1993) 258.
[27] H. Masui, Ph.D. Dissertation, York University, Toronto, Ontario, Canada, 1994, p. 158.
[28] H. Masui, A.L. Freda, A.B.P. Lever, Inorg. Chem. 39 (2000) 141.

[29] R.A. Metcalfe, A.B.P. Lever, Inorg. Chem. 36 (1997) 4762.
[30] R.A. Metcalfe, L.C.G. Vasconcellos, H. Mirza, D.W. Franco, A.B.P. Lever, J. Chem. Soc. Dalton Trans. (1999) 2653.
[31] R.A. Metcalfe, E.S. Dodsworth, S.S. Fielder, D.J. Stufkens, A.B.P. Lever, W.J. Pietro, Inorg. Chem. 35 (1996) 7741.
[32] R.A. Metcalfe, E.S. Dodsworth, A.B.P. Lever, W.J. Pietro, D.J. Stufkens, Inorg. Chem. 32 (1993) 3581.
[33] C.J. Cunha, E.S. Dodsworth, A.B.P. Lever, Inorg. Chim. Acta 242 (1996) 293.
[34] C.J. da Cunha, E.S. Dodsworth, M.A. Monteiro, A.B.P. Lever, Inorg. Chem. 38 (1999) 0000.
[35] S.I. Gorelsky, E.S. Dodsworth, A.A. Vlcek, A.B.P. Lever, Coord. Chem. Rev. 174 (1998) 469.
[36] R.G. Parr, Quantum Theory of Molecular Electronic Structure, W.A. Benjamin, New York, 1963.
[37] A. Szabo, N.S. Ostlund, Modern Quantum Chemistry, Macmillan, New York, 1982.
[38] A.B.P. Lever, E.I. Solomon, Electronic Structure, Spectroscopy, vol. 1, Wiley, New York, 1999, p. 1.
[39] W.P. Anderson, T. Cundari, R.S. Drago, M.C. Zerner, Inorg. Chem. 29 (1989) 1.
[40] M.C. Zerner, Int. J. Quant. Chem. 35 (1989) 567.
[41] W.D. Edwards, M.C. Zerner, Theor. Chim. Acta 72 (1987) 347.
[42] A.D. Bacon, M.C. Zerner, Theor. Chim. Acta 53 (1979) 21.
[43] M.C. Zerner, Metal–Ligand Interactions, Kluwer, The Netherlands, 1996, p. 493.
[44] J.C. Culberson, P. Knappe, N. Rösch, M.C. Zerner, Theor. Chim. Acta 71 (1987) 21.
[45] C. Martin, M.C. Zerner, in: E.I. Solomon, A.B.P. Lever (Eds.), Inorganic Electronic Structure and Spectroscopy, vol. 1, Wiley, New York, 1999, p. 555.
[46] J. Ridley, M.C. Zerner, Theor. Chim. Acta 32 (1973) 111.
[47] J. Ridley, M.C. Zerner, Theor. Chim. Acta 42 (1976) 223.
[48] M.C. Zerner, G.H. Loew, R.F. Kirchner, U.T. Mueller-Westerhoff, J. Am. Chem. Soc. 102 (1980) 589.
[49] W.P. Anderson, W.D. Edwards, M.C. Zerner, Inorg. Chem. 25 (1986) 2728.
[50] K. Krogh-Jespersen, J.D. Westbrook, J.A. Potenza, H.J. Schugar, J. Am. Chem. Soc. 109 (1987) 7025.
[51] K. Krogh-Jespersen, X. Zhang, J.D. Westbrook, R. Fikar, K. Nayak, W.-L. Kwik, J.A. Potenza, H.J. Schugar, J. Am. Chem. Soc. 111 (1989) 4082.
[52] K. Krogh-Jespersen, X. Zhang, Y. Ding, J.D. Westbrook, J.A. Potenza, H.J. Schugar, J. Am. Chem. Soc. 114 (1992) 4345.
[53] W.P. Anderson, T. Cundari, M.C. Zerner, Int. J. Quant. Chem. 39 (1991) 31.
[54] H. Kobayashi, Y. Kaizu, Coord. Chem. Rev. 64 (1985) 53.
[55] A. Juris, V. Balzani, P. Belser, A. von Zelewsky, Helv. Chim. Acta 64 (1981) 2175.
[56] R.J. Crutchley, A.B.P. Lever, J. Am. Chem. Soc. 102 (1980) 7128.
[57] L.F. Warren, Inorg. Chem. 16 (1977) 2814.
[58] Calculations individually involved determining the excitation energies for HOMO → LUMO, HOMO-1 → LUMO, HOMO → LUMO and LUMO + 1,2 etc. which allowed the energies of specific states to be determined in isolation from others with which they might couple. Use was also made of the property of a matrix such that the trace is constant. Thus, for example, the sum of the three calculated E transitions is a constant irrespective of whether the mixed or unmixed E states are considered. For degenerate e → e transitions, the singlet-triplet separation is not $2K$, but has additional terms [59]. These states are omitted form this analysis.
[59] C. Dual. Baerends, P. Vernooijs, Inorg. Chem. 33 (1994) 3538.